

Enhancement Performance of CdSe Quantum Dot Based Solar Cells Influence of Graphene Nanoparticles

Ali Rasad

Department of Physics, Urmia University, Urmia, Iran

Email address:

rasadph7@gmail.com

To cite this article:

Ali Rasad. Enhancement Performance of CdSe Quantum Dot Based Solar Cells Influence of Graphene Nanoparticles. *American Journal of Physics and Applications*. Vol. 10, No. 3, 2022, pp. 51-56. doi: 10.11648/j.ajpa.20221003.11

Received: June 28, 2022; **Accepted:** July 28, 2022; **Published:** August 4, 2022

Abstract: Recently, Quantum dot-based solar cells (QDSCs) as the third-generation solar cell are attracting considerable attention in many photovoltaic researches. CdSe quantum dots (or nanocrystals) have been exploited in many studies as inorganic dye to sensitize TiO_2 thin films in QDSCs due to their unique properties for harvesting energy and enhancement efficiency in converting solar energy to electricity. As yet, various researches have been conducted with different results in order to increase the efficiency of this type of solar cells. This paper reports investigation of the influence of 2 wt.% graphene nanoparticles in the TiO_2 semiconductor layer on the performances of CdSe-QDCs. At 1 sun illumination condition, the efficiency η ranged from 0.03 to 0.11%. Also, obtained results showed reduction the parasitic resistances effects such as series and shunt resistances. The electron diffusion coefficient D_n and lifetime τ_n are determined from the non-linear least squares fitting method at open circuit voltage decay under the Nd:YAG laser pulses. The results and analysis from measurements show increasing the D_n , τ_n , electron mobility μ , and diffusion length L_n . As the result, investigations indicative the reduction of recombination centers due to specific electrical properties of the graphene nanoparticles and improvement performance of this type of solar cell.

Keywords: Quantum Dot, CdSe, Graphene, Solar Cell

1. Introduction

Greenhouse gases emission is one of the irreparable effects of human activities in the use of unrenewable energy resources such as fossil fuels, principally coal, oil, and natural gas [1, 2]. In most countries, many scientific efforts have been proposed to decrease these effects. In recent years, photovoltaic PV solar cells meet an important and effective role in the world for generating electrical energy and decreasing dependency on unrenewable resources [3, 4].

Due to the ability to overcome the Shockley-Queisser limit, the third generation solar cells like quantum dot-based solar cells QDSC have been more studied than other types of them [5, 6]. Up to 66% in photon conversion efficiency to produce higher photo-voltages or higher photo-current caused to increase the attentions to QDSCs [7]. Quantum dots due to some advantages such as multiple-exciton-generation MEG [8], wide sun spectrum absorption by size variation, high carrier lifetime, and diffusion coefficient [9] are utilized in a wide range of applications including solar

cells, transistors, medical imaging, quantum computing, light emitting diodes LEDs [10]. Tunable the band gap and easily fabrication method in desired dimensions caused to the various quantum dots such as CdTe, CdS, CdSe, etc have been used as a sensitizer for harvesting energy in QDSCs that among them, CdSe has attracted more attention due to its high quantum efficiency [11-13].

Parasitic resistances such as series resistance R_s and shunt resistance R_{sh} can reduce the efficiency of the solar cell. These resistances reduce the fill factor without effect on the open circuit voltage V_{oc} and short circuit current I_{sc} (Figure 1). The flux of the current through the semiconductor materials used in solar cells, the resistance of contact between the semiconductor and metal, and the resistance of the metal contacts on both sides of solar cells caused appearance of the series resistance. High R_s or low R_{sh} caused power losses and reduced the efficiency of solar cells. The reduction of R_{sh} causes to decrease in the power in solar cells due to the created defects in the manufacturing process and this is by creating an alternate path for light-generated current [14, 15].

Graphene as the two-dimensional allotrope of carbon consisting of a single layer of carbon atoms with sp^2 hybridization and hexagonal lattice structure is employed in most investigations due to its exclusive properties such as high heat and electrical conductivity, high electron and hole mobility, high specific surface area, etc [16].

The effects of graphene on the performance of the CdSe-QDSC have been presented in this paper. For this aim, graphene-treated sample and initial sample were tested under sun illumination (STC) and laser pulses (lab environment conditions), and their results were investigated.

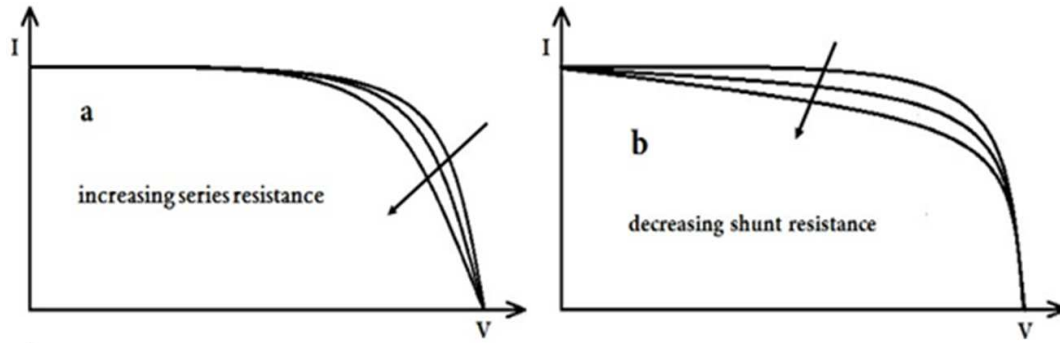


Figure 1. Effects of shunt and series resistances on the: a) open circuit voltage and b) short circuit current.

2. Materials and Methods

The 2×2 fluorine-doped tin oxide FTO substrates for use as anode electrodes were cleaned with acetone and distilled water by using an ultrasonic cleaner for 45s. 0 and 2 wt.% of graphene ink were added in TiO_2 sol and were coated on FTO substrates by spin coating method in ambient conditions (rpm: 1600, time: 60s) and then, TiO_2 paste (in anatase phase) were coated on the substrates by Dr-Blade method. Substrates were heated in a furnace at 450 c for 25 min and these substrates were plunged in CdSe quantum dots solution for 24 hours. On other hand and for cathode sides, the platinum paste was coated on the FTO substrates and heated like anode electrodes. Polysulfide electrolyte is a general choice for application in QDSCs. To assemble the solar cells, some drops of the polysulfide electrolyte were decanted on the anode substrates and cathode electrodes were placed on them, directly. (Figure 2).

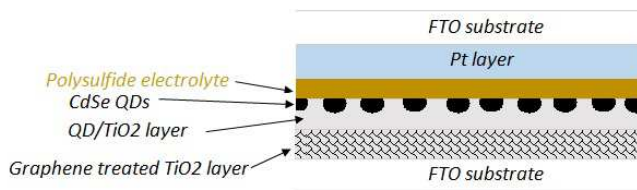


Figure 2. The schematic diagram of graphene-treated CdSe-QDSC.

3. Results and Discussion

The SEM images of presence of the graphene in the TiO_2 semiconductor layer were presented in Figure 3.

In the first, samples were tested under sun illumination and standard conditions (100 mW/cm^2 , AM 1.5G). Enhancement of the efficiency due to the presence of graphene nanoparticles was confirmed by the J-V curves reported in Figure 4a.

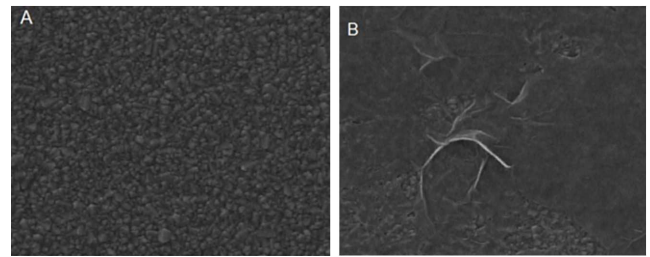


Figure 3. The SEM analysis images of presence of the graphene in the TiO_2 semiconductor layer of A) the initial CdSe-QDSC sample and B) the graphene-treated CdSe-QDSC sample.

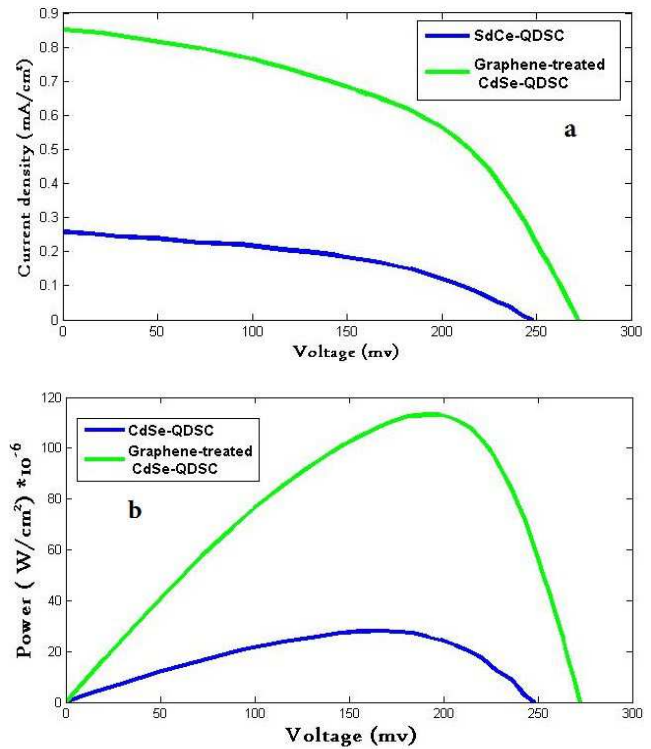


Figure 4. a) J-V and b) P-V characteristics of initial (blue line) and graphene-treated sample (green line) of CdSe-QDSC.

The fill factor FF and the efficiency η of the solar cell are given by:

$$FF = \frac{J_m V_m}{J_{sc} V_{oc}} \quad (1)$$

$$\eta_{\%} = \frac{J_{sc} V_{oc} \times FF}{P_{in}} \times 100 \quad (2)$$

Where, P_{in} is the intensity of incident light, J_m and V_m represented the current density and voltage in the maximum

power point MPP of the J-V curve.

As shown in Table 1, photocurrent density of 0.257 mA/cm², V_{oc} of 248.2 mv, FF of 44.07% increased to 0.851 mA/cm², 272.1 mv, 48.88%, respectively. As a result, CdSe-QDSC efficiency is improved by about 3.6%. Increasing the MPP of the grapheme-treated cell is another reason for enhancing external efficiency as shown by the power-voltage P-V curves in Figure 4b.

Table 1. Obtained values from J-V characteristics of samples.

Sample	J_{sc} (mA/cm ²)	V_{oc} (mv)	FF (%)	η (%)
CdSe-QDSC	0.257	248.2	44.07	0.03
Graphene-treated CdSe-QDSC	0.851	272.1	48.88	0.11

The equivalent electrical circuit of the solar cell was shown in Figure 5. Based on this model, the theoretical relation between current I and voltage V is given by [17]:

$$I = I_{ph} - I_0 \left[\exp \left(\frac{V + IR_s}{mV_{th}} \right) - 1 \right] - \frac{V + IR_s}{R_{sh}} \quad (3)$$

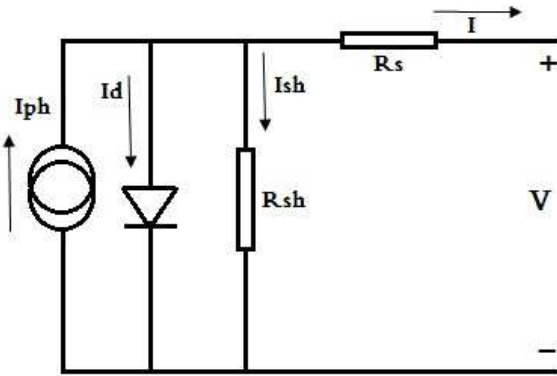


Figure 5. The theoretical equivalent circuit of a solar cell contains shunt and series resistances.

Where I_0 is the reverse saturation dark current of the solar cell, I_{ph} is the photo-generated current and V_{th} is the thermal voltage that in room temperature $V_{th}=26$ mv. On other hand, I_{ph} and I_0 can be written as [18]:

$$I_{ph} = [I_{sc} + K_i(T - T_r)] \frac{S}{100} \quad (4)$$

$$I_0 = I_r \left(\frac{T}{T_r} \right)^3 \exp \left[\frac{qE_g}{mk} \left(\frac{1}{T_r} - \frac{1}{T} \right) \right] \quad (5)$$

$$I_r = \frac{I_{sc}}{\exp \left(\frac{V_{oc}}{mV_{th}} \right) - 1} \quad (6)$$

where K_i is the short circuit current temperature coefficient, S is the solar radiation, T_r is the reference temperature, E_g is the semiconductor band gap and I_r is the cell's reverse saturation current at solar radiation.

Many methods have been used to determine the parasitic resistances [19]. In one case, the R_s and R_{sh} obtained from the measurement slopes of the I-V curve at the short circuit current point ($I = I_{sc}$) and the open circuit voltage point ($V = V_{oc}$) [20]:

$$R_s = - \left(\frac{dV}{dI} \right)_{V=V_{oc}} \quad (7)$$

$$R_{sh} = - \left(\frac{dV}{dI} \right)_{I=I_{sc}} \quad (8)$$

The simple linear fit was employed for these measurements that is shown in Figure 6.

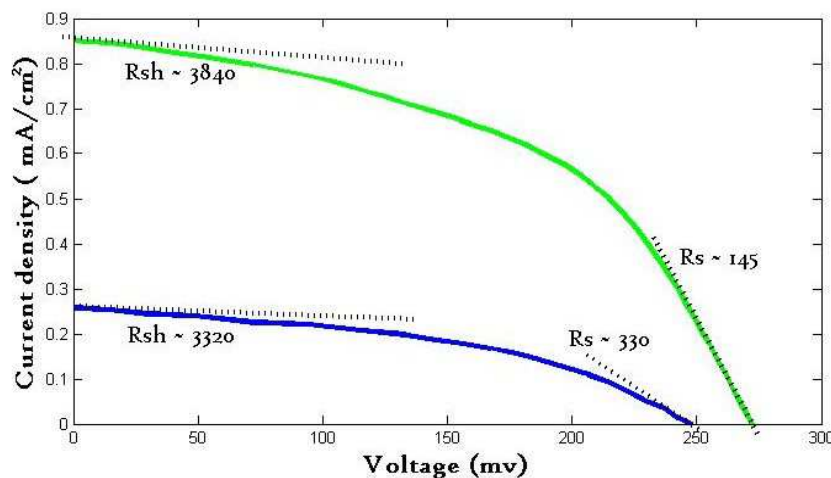


Figure 6. Shunt and series resistances measurements from slopes of J-V curves for both samples. For the initial sample, R_s and R_{sh} obtained 330 and 3320 Ω that for grapheme-treated sample obtained 145 and 3840 Ω , respectively.

Obtained values for R_s and R_{sh} from the measurements indicate the reduction of parasitic resistances effects due to the presence of graphene in the semiconductor layer. In the presence of the R_s and R_{sh} the FF expression by:

$$FF' = FF(1 - R_s)(1 - \frac{1}{R_{sh}}) \quad (9)$$

Where the FF and FF' represented the initial and final fill factor. Reduction of the parasitic resistances effects caused improvement the fill factor and then enhancement of the efficiency of solar cell [14, 15]. In the ideal model for solar cells: $R_s \rightarrow 0$ and $R_{sh} \rightarrow \infty$.

In order to investigate the electron lifetime and diffusion coefficient in the cells, a second harmonic output of a Q-Switched Nd:YAG (Brio, Quanta Inc) with the wavelength of 532 nm was used. The nominal width and energy of the laser pulses were 5 ns and 85 mj, respectively. The open circuit voltage decay OCVD to evaluate the charge recombination in samples was performed. Figure 7 shows exponential decay after the interruption of the laser pulses. Slower exponential decay (graphene-treated sample) shows the enhancement of the charge lifetime.

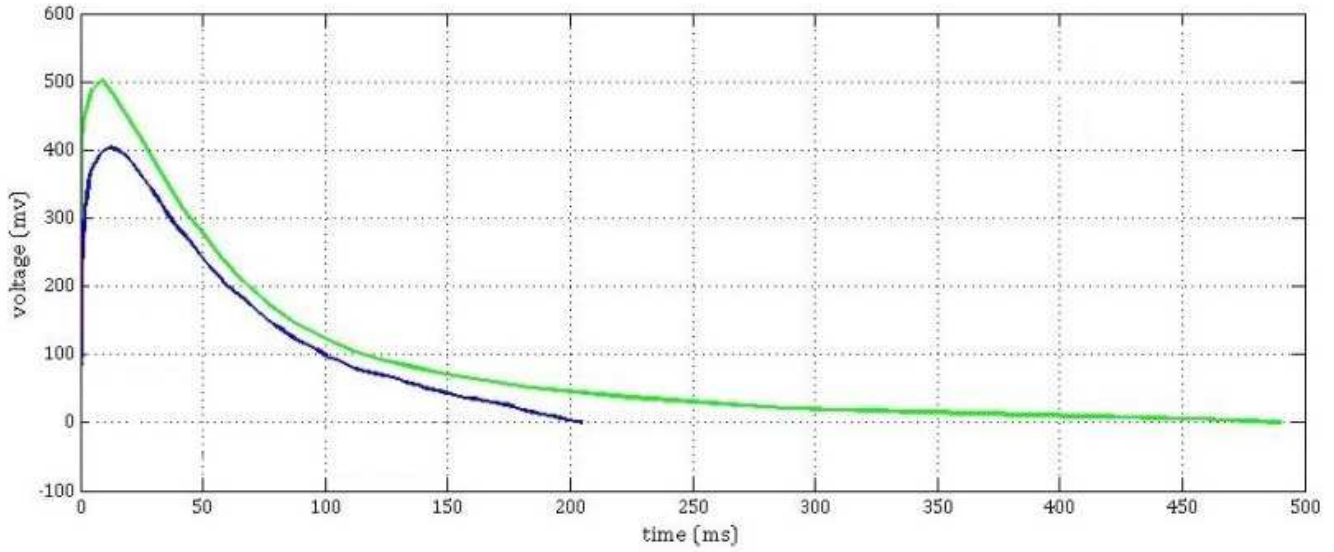


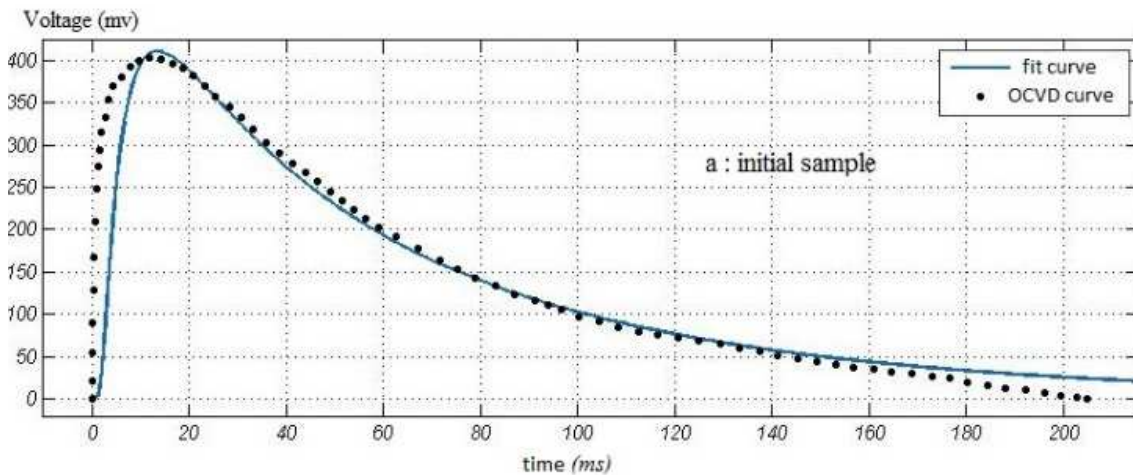
Figure 7. Open circuit voltage decay curves of initial (blue) and graphene treated (green) samples after interruption laser pulses.

For more analysis, by a powerful method, the experimentally measured OCVD data were fitted (Figure 8) using the below equation with non-linear least squares fitting [21, 22]:

$$\Delta V(t) = \frac{\Delta Q_{ini} d}{C_{TiO_2} \sqrt{\pi D_n t}} \exp\left(-\frac{t}{\tau_n}\right) \sum_{g=0}^{\infty} \left\{ \exp\left(-\frac{(-(1+2g)d)^2}{4D_n t}\right) + \exp\left(-\frac{((1+2g)d)^2}{4D_n t}\right) \right\} \quad (10)$$

Where ΔQ_{ini} is excess charge in the semiconductor layer initially injected by perturbation, t is time, and C_{TiO_2} is the chemical capacitance of the TiO_2 layer. Four terms in the series ($g = 0, 1, 2, 3$) were used for the fit in the equation although two

terms ($g = 0, 1$) are necessary. The charge carrier's lifetime τ_n and diffusion coefficient D_n can be determined with this method by minimum error. As shown in Table 2, D_n and τ_n were increased for the graphene-treated sample.



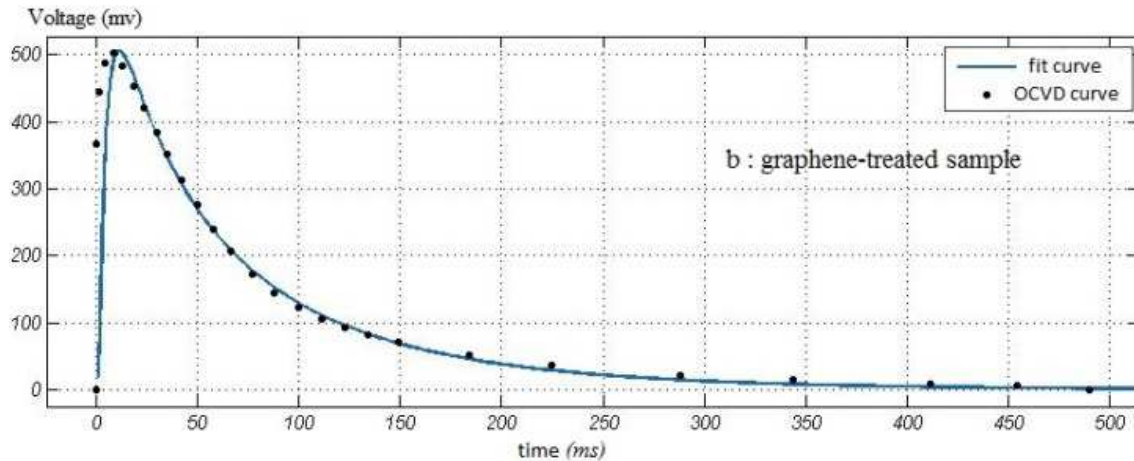


Figure 8. The modeled of transients with non-linear least squares fitting method by 95% confidence bonds for a) initial sample and b) graphene-treated sample.

Table 2. Obtained values for D_n and τ_n from fit to OCVD curves for both samples.

Sample	$\frac{\Delta Q_{int}}{C_{TiO_2}} (mv)$	$\tau_n (ms)$	$D_n (m^2/s)$
CdSe-QDSC	469	92	6.5 e-9
Graphene-treated CdSe-QDSC	639	110	8.3 e-9

Diffusion length L_n is the average length of a minority carrier from generation point until recombination that can expression by [23]:

$$L_n = \sqrt{D_n \tau_n} \quad (11)$$

Increasing the L_n indicative reduction of recombination probability of the minority carriers. Also, high carrier mobility allows to the high exploitation of photo-generated minority carriers. Charge carrier's mobility μ given by

Einstein equation as $\mu = \left(\frac{1}{V_{th}} \right) D_n$ [24]. An enhancement for L_n and μ was obtained according to measurement values in Table 3.

Table 3. Measured values of L_n and μ for samples.

Sample	$L_n (\mu m)$	$\mu (m^2/v.s)$
CdSe-QDSC	24.45	0.25 e-6
Graphene-treated CdSe-QDSC	30.22	0.32 e-6

As another result, the presence of the graphene in the TiO_2 semiconductor layer due to its exclusive electrical properties and sp^2 hybridization caused to increasing velocity of transmission of the minority carriers and diffusion coefficient that caused the reduction of the recombination centers and enhancement of the minority carrier's lifetime.

4. Conclusion

In summary, CdSe-based QDSC affected graphene nanoparticles under 1 sun illumination STC and Nd:YAG laser pulses were tested, and performance of the both samples was investigated. An enhancement efficiency of 3.6% and

reduction of parasitic resistances effects were achieved in the CdSe-QDSC sample fabricated using the 2 wt.% graphene in the semiconductor layer in STC. Other studies under laser pulses for minority carrier lifetime, diffusion coefficient, diffusion length, and minority charge carriers indicated the reduction of recombination trap density due to the graphene nanoparticles coverage led to the rapid diffusion of the photo-generated minority carriers. In order to more accurately investigate the effect of graphene nanoparticles on the performance of this type of solar cells, in the next experiments, different percentages of this material can be exploited in the semi-conducting layer and the results examined in each sample.

References

- [1] Reddy, K. Govardhan, et al. "On global energy scenario, dye-sensitized solar cells and the promise of nanotechnology." *Physical Chemistry Chemical Physics* 16. 15 (2014): 6838-6858.
- [2] Garcia-Rodríguez, Rodrigo, et al. "A Critical Evaluation of the Influence of the Dark Exchange Current on the Performance of Dye-Sensitized Solar Cells." *Materials* 9. 1 (2016): 33.
- [3] Mitzi, David B., et al. "The path towards a high-performance solution-processed kesterite solar cell." *Solar Energy Materials and Solar Cells* 95. 6 (2011): 1421-1436.
- [4] Price, Selya. "2008 solar technologies market report." (2010).
- [5] Green, Martin A. "Third generation photovoltaics: solar cells for 2020 and beyond." *Physica E: Low-dimensional Systems and Nanostructures* 14. 1-2 (2002): 65-70.
- [6] Nozik, Arthur J., et al. "Semiconductor quantum dots and quantum dot arrays and applications of multiple exciton generation to third-generation photovoltaic solar cells." *Chemical reviews* 110. 11 (2010): 6873-6890.
- [7] Nozik, A. J. "Quantum dot solar cells." *Physica E: Low-dimensional Systems and Nanostructures* 14. 1-2 (2002): 115-120.

- [8] Luque, Antonio, Antonio Martí, and Arthur J. Nozik. "Solar cells based on quantum dots: multiple exciton generation and intermediate bands." *MRS bulletin* 32. 3 (2007): 236-241.
- [9] Carey, Graham H., et al. "Colloidal quantum dot solar cells." *Chemical reviews* 115. 23 (2015): 12732-12763.
- [10] Straus, Daniel B., et al. "Increased Carrier Mobility and Lifetime in CdSe Quantum Dot Thin Films through Surface Trap Passivation and Doping." *The journal of physical chemistry letters* 6. 22 (2015): 4605-4609.
- [11] Bang, Jin Ho, and Prashant V. Kamat. "Quantum dot sensitized solar cells. A tale of two semiconductor nanocrystals: CdSe and CdTe." *ACS nano* 3. 6 (2009): 1467-1476.
- [12] Fuke, Nobuhiro, et al. "CdSe quantum-dot-sensitized solar cell with ~ 100% internal quantum efficiency." *Acs Nano* 4. 11 (2010): 6377-6386.
- [13] Kongkanand, Anusorn, et al. "Quantum dot solar cells. Tuning photoresponse through size and shape control of CdSe–TiO₂ architecture." *Journal of the American Chemical Society* 130. 12 (2008): 4007-4015.
- [14] Green, Martin A. "Solar cells: operating principles, technology, and system applications." *Englewood Cliffs, NJ, Prentice-Hall, Inc., 1982. 288 p.* (1982).
- [15] Dieme, Nfally, and Moustapha Sane. "Impact of Parasitic Resistances on the Output Power of a Parallel Vertical Junction Silicon Solar Cell." *Energy and Power Engineering* 8. 03 (2016): 130.
- [16] Neto, AH Castro, et al. "The electronic properties of graphene." *Reviews of modern physics* 81. 1 (2009): 109.
- [17] Anku, Nerissa EL, et al. "A model for photovoltaic module optimisation." *Journal of Mechanical Engineering and Automation* 5. 2 (2015): 72-79.
- [18] Tsai, Huan-Liang, Ci-Siang Tu, and Yi-Jie Su. "Development of generalized photovoltaic model using MATLAB/SIMULINK." *Proceedings of the world congress on Engineering and computer science*. Vol. 2008. 2008.
- [19] Cotfas, Daniel T., et al. "The methods to determine the series resistance and the ideality factor of diode for solar cells-review." *Optimization of Electrical and Electronic Equipment (OPTIM), 2012 13th International Conference on*. IEEE, 2012.
- [20] Ishibashi, Ken-ichi, Yasuo Kimura, and Michio Niwano. "An extensively valid and stable method for derivation of all parameters of a solar cell from a single current-voltage characteristic." *Journal of applied physics* 103. 9 (2008): 094507.
- [21] Barnes, Piers RF, et al. "Interpretation of optoelectronic transient and charge extraction measurements in dye-sensitized solar cells." *Advanced materials* 25. 13 (2013): 1881-1922.
- [22] Nakade, S., et al. "Laser-induced photovoltage transient studies on nanoporous TiO₂ electrodes." *The Journal of Physical Chemistry B* 108. 5 (2004): 1628-1633.
- [23] Bisquert, Juan, et al. "Electron lifetime in dye-sensitized solar cells: theory and interpretation of measurements." *The Journal of Physical Chemistry C* 113. 40 (2009): 17278-17290.
- [24] Tiwana, Priti, et al. "Electron mobility and injection dynamics in mesoporous ZnO, SnO₂, and TiO₂ films used in dye-sensitized solar cells." *ACS nano* 5. 6 (2011): 5158-5166.